THE JOURNAL OF BIOLOGICAL CHEMISTRY VOL. 284, NO. 42, pp. 28498–28509, October 16, 2009
Printed in the U.S.A.

A Novel Pathway of Insulin Sensitivity in Chromogranin A Null Mice

*A CRUCIAL ROLE FOR PANCREASTATIN IN GLUCOSE HOMEOSTASIS**

Received for publication, May 13, 2009, and in revised form, July 23, 2009 Published, JBC Papers in Press, August 25, 2009, DOI 10.1074/jbc.M109.020636

Jiaur R. Gayen[‡], Maziyar Saberi[‡], Simon Schenk[‡], Nilima Biswas[‡], Sucheta M. Vaingankar[‡], Wai W. Cheung[§], Sonia M. Najjar[¶], Daniel T. O'Connor[‡‖], Gautam Bandyopadhyay[‡], and Sushil K. Mahata[‡**1]**

*From the Departments of [‡]Medicine, [§]Pediatrics, and [‖]Molecular Genetics, University of California, San Diego and **Veterans Affairs San Diego Healthcare System, La Jolla, California 92093-0838 and the [¶]Center for Diabetes and Endocrine Research and Department of Physiology and Pharmacology, University of Toledo College of Medicine, Toledo, Ohio 43614-5804*

Chromogranin A (CHGA/Chga), a proprotein, widely distributed in endocrine and neuroendocrine tissues (not expressed in muscle, liver, and adipose tissues), generates at least four bioactive peptides. One of those peptides, pancreastatin (PST), has been reported to interfere with insulin action. We generated a Chga knock-out (KO) mouse by the targeted deletion of the *Chga* gene in neuroendocrine tissues. KO mice displayed hypertension, higher plasma catecholamine, and adipokine levels and lower IL-6 and lipid levels compared with wild type mice. Liver glycogen content was elevated, but the nitric oxide (NO) level was diminished. Glucose, insulin, and pyruvate tolerance tests and hyperinsulinemic-euglycemic clamp studies established increased insulin sensitivity in liver but decreased glucose disposal in muscle. Despite higher catecholamine and ketone body levels and muscle insulin resistance, KO mice maintained euglycemia due to increased liver insulin sensitivity. Suppressed mRNA abundance of phosphoenolpyruvate carboxykinase and glucose-6-phosphatase (G6Pase) in KO mice further support this conclusion. PST administration in KO mice stimulated phosphoenolpyruvate carboxykinase and G6Pase mRNA abundance and raised the blood glucose level. In liver cells transfected with G6Pase promoter, PST caused transcriptional activation in a protein kinase C (PKC)- and NO synthase-dependent manner. Thus, PST action may be mediated by suppressing IRS1/2-phosphatidylinositol 3-kinase-Akt-FOXO-1 signaling and insulin-induced maturation of SREBP1c by PKC and a high level of NO. The combined effects of conventional PKC and endothelial NO synthase activation by PST can suppress insulin signaling. The rise in blood PST level with age and in diabetes suggests that PST is a negative regulator of insulin sensitivity and glucose homeostasis.

Chromogranin A (CHGA/Chga),[2] the index member of the chromogranin/secretogranin protein family (1, 2), is a proprotein that gives rise to biologically active peptides such as the dysglycemic hormone pancreastatin (PST; human CHGA-(250–301)) (3), the vascular smooth muscle vasodilator vasostatin (human CHGA-(1–76)) (4), and a catecholamine release inhibitory peptide, catestatin (human CHGA-(352–372); bovine Chga-(344–364)) (5). Several studies, including *in vivo* analyses of experimental animals (6, 7), showed that PST inhibits insulin release in response to glucose (3), reduces glucose uptake in adipocytes and hepatocytes (8), and triggers glycogenolysis (6). Genetic analysis in humans supports a role for PST in decreasing glucose uptake by ~50% (9) while increasing the spillover of free fatty acids but not amino acids. Moreover the PST level is elevated in patients with Type 2 diabetes mellitus (9–11). Taken together, the data suggest that PST is an important player in metabolism.

To further delineate the role of PST in metabolism, we tested whether removal of PST, a negative regulator of insulin action, stabilizes glucose levels in knock-out (KO) mice and protects against metabolic disorders. To this end, we characterized more extensively the phenotype of the global *Chga* KO mouse (12), which we had found to be hypertensive (resulting from elevation in catecholamine release) and hyperadrenergic (12). We herein report that by comparison with wild type (WT), KO mice are euglycemic despite low plasma insulin levels. Contrary to what is found in hypertension (13), hypertensive KO mice exhibited a high plasma adiponectin level.

EXPERIMENTAL PROCEDURES

Animals—Young adult (3 months old) and adult (6 months old) WT (31 ± 1 g) and KO (37 ± 1 g) mice with mixed genetic

* This work was supported, in whole or in part, by National Institutes of Health Grants R01 DA011311 (to S. K. M.), DK60702 (to D. T. O.), P01 HL58120 and U01 HL69758 (to S. K. M. and D. T. O.), and DK54254 (to S. M. N.). This work was also supported by grants from the Department of Veterans Affairs (to S. K. M. and D. T. O.) and United States Department of Agriculture Grant USDA 38903-02315 (to S. M. N.).

[1] To whom correspondence should be addressed: Dept. of Medicine (0838), University of California, San Diego School of Medicine and Veterans Affairs San Diego Healthcare System, 9500 Gilman Dr., La Jolla, CA 92093-0838. Tel.: 858-552-8585 (ext. 2637) or 858-534-0639; Fax: 858-642-6425; E-mail: smahata@ucsd.edu.

[2] The abbreviations used are: CHGA/Chga, human/mouse chromogranin A; *CHGA*/*Chga*, human/mouse chromogranin A gene; Akt, serine/threonine kinase; *Fasn*, fatty-acid synthase gene; FOXO-1, the forkhead transcription factor; *Gpat*, glycerol-3-phosphate acyltransferase gene; G6Pase, glucose-6-phosphatase; *G6pase*, glucose-6-phosphatase gene; KO, knock-out; GTT, glucose tolerance test; IRS, insulin receptor substrate; ITT, insulin tolerance test; NEFA, non-esterified fatty acid; *Pepck1*, phosphoenolpyruvate carboxykinase-1 gene; *Pparγ*, peroxisome proliferator-activated receptor γ gene; PKC, protein kinase C; cPKC, conventional PKC; PST, pancreastatin; SREBP1c, sterol-regulatory element-binding protein 1c; *Srebp1c*, sterol-regulatory element-binding protein 1c gene; *Ucp2*, uncoupling protein 2 gene; WT, wild type; NO, nitric oxide; GDR, glucose disposal rate; PI, phosphatidylinositol; cPI, cPKC peptide inhibitor; ANOVA, analysis of variance; NOS, nitric-oxide synthase; eNOS, endothelial NOS.

background (129svJ × C57BL/6) were used in this study. Both WT and KO mice were generated from the original founder carrying mixed genotype (50% 128svJ, 50% C57BL/6) and were maintained by brother/sister mating. Animals were kept in a 12-h dark/light cycle and fed standard chow *ad libitum*. The Institutional Animal Care and Utilization Committee approved all procedures. Equal numbers of male and female mice were fasted overnight (12 h) for each experiment except for the clamp study where only male mice were used.

Dual Energy X-ray Absorptiometry Scan—Following anesthesia with isoflurane, overnight fasted mice underwent dual energy x-ray absorptiometry scanning to measure total tissue and fat mass and lean body mass using a PixiMus mouse densitometer (GE Healthcare).

Measurement of Blood Glucose, Insulin, C-peptide, Glucagon, Adipokine, Lipid, Cytokine, and PST Levels in Fasted Mice—Blood glucose was measured using microcuvettes (HemoCue, Lake Forest, CA) and a Glucose 201 analyzer (HemoCue). A mouse insulin enzyme-linked immunosorbent assay kit (Millipore, Billerica, MA) was used to determine plasma insulin. C-peptide was measured using an enzyme-linked immunosorbent assay kit (Shibayagi Co. Ltd.). Glucagon was measured using an enzyme-linked immunosorbent assay kit (Wako Chemicals). A radioimmunoassay kit (Peninsula Laboratories, San Carlos, CA) was used to measure plasma PST. Plasma triglyceride and non-esterified fatty acid (NEFA) levels were assayed by triacylglycerol and NEFA C test kits, respectively, from Wako Diagnostics (Richmond, VA). Enzyme-linked immunosorbent assay kits were used to determine plasma levels of leptin and adiponectin (Millipore) and IL-6 (Pierce).

Blood Ketone (β-Ketone) Assay—The blood (tail snip) ketone level (mmol/liter) was measured using the Precision Xtra Blood Ketone Monitoring System (Abbott Laboratories) according to manufacturer's instructions.

Determination of Liver Glycogen and NO Content—Liver tissue (25–100 mg) was dissolved in hot KOH (30%) before glycogen was precipitated in 3 ml of 95% ethanol (at 4 °C overnight) and centrifuged at 5000 rpm for 12 min. The pellet was redissolved in 5 ml of water, and 1 ml was mixed with 3 ml of anthrone reagent (0.2% anthrone (Sigma) in concentrated H_2SO_4) (14) to determine the concentration at 620 nm by comparison with standard glycogen (Sigma). A nitrate/nitrite colorimetric assay kit (Cayman Chemical Co.) was used to determine liver NO content.

Glucose, Insulin, and Pyruvate Tolerance Tests—Dextrose (2 g/kg intraperitoneally; glucose tolerance test (GTT)), human insulin (0.40 IU/kg intraperitoneally; Novolin, Novo Nordisk Inc.; insulin tolerance test (ITT)), or pyruvate (2 g/kg intraperitoneally; pyruvate tolerance test) were injected into fasting (12 h) mice before determining the tail vein glucose level at 0–150 min following injection.

Hyperinsulinemic-Euglycemic Clamp—Briefly mice were anesthetized (80 mg/kg ketamine, 0.5 mg/kg acepromazine, and 16 mg/kg xylazine) via intramuscular injection. Two microurethane catheters (0.012-μm inner diameter; Dow Corning Silastic) were inserted in the jugular vein, and the cannulas were externalized to the midscapula region and secured within tubing. After 5 days of recovery, mice were fasted (3 h) and placed in a Lucite restrainer (Braintree Scientific, Braintree, MA). After 90 min, an equilibrating tracer solution of D-[3-^{3}H]glucose (5 μCi/h; PerkinElmer Life Sciences) was infused via the jugular cannula for 90 min. At the end of the equilibration period ($t = 0$ min; fasted for 6 h), blood was collected (15 μl in duplicate) and deproteinized to assess tracer specific activity and basal hepatic glucose production. In addition, ~75 μl of whole blood was collected by cutting the tail vein for the measurement of fasting plasma insulin and free fatty acid concentrations. After blood collection, mice were infused with insulin (12.0 milliunits/kg/min; Humulin® R, Eli Lilly and Co.) and D-[3-^{3}H]glucose (5 μCi/h; PerkinElmer Life Sciences). Blood glucose was assessed every 10 min, and a glucose solution (50% dextrose; Hospira, Inc.) was infused at a variable rate to maintain blood glucose at ~120 ± 5 mg/dl. The clamp was terminated when steady state conditions were maintained for ≥30 min (~130 min). At this time, blood was sampled (15 μl in duplicate) 10 min apart to assess glucose disposal rate (GDR) and insulin-stimulated hepatic glucose production and to verify that steady state conditions for specific activity of the tracer were achieved. An additional 75 μl of whole blood was also collected at the end of the clamp to measure plasma insulin and free fatty acids concentrations during the clamp.

Glucose Production in Primary Hepatocytes—Mice were infused with collagenase (Blendzyme, Roche Applied Science) through the inferior vena cava, and hepatocytes were isolated by the method of Smedsrød and Pertoft (15). Percoll-purified hepatocytes were cultured in William's medium E (Invitrogen), 2 mM Glutamax, 10 nM dexamethasone, 5% fetal calf serum, and antibiotics. Dexamethasone was withdrawn 6 h later, and cultures were exposed initially to PST (20 nM) for 20 h and then to glucose-free, serum-free Dulbecco's modified Eagle's medium containing PST for an additional 4 h. Dulbecco's modified Eagle's medium was then replaced by phosphate-buffered saline containing 20 mM HEPES, 0.2% bovine serum albumin, 16 mM lactate, and 4 mM pyruvate with or without insulin (20 nM) and incubated for another 4 h. At the end, glucose levels in the media were assayed by a kit (Cayman Chemicals, Ann Arbor, MI), and cellular protein levels were determined by the Bradford assay (Bio-Rad).

Primary Adipocytes and L6 Muscle Cell Cultures—Adipocytes were isolated from mouse visceral adipose tissue following a procedure described by Karnieli *et al.* (16). L6 muscle cells were obtained from the laboratory of Dr. A. Klip (Hospital for Sick Children, Toronto, Canada). L6 myoblast cells were grown in α-minimum Eagle's medium supplemented with 10% fetal bovine serum and then switched to 2% fetal bovine serum for differentiation into myotubes. After 8 days in differentiation medium, myotubes were used for glucose uptake studies. Glucose uptake in muscle and adipocytes cells was carried out in HEPES-salt buffer with or without 20 nM insulin treatment for 30 min followed by incubation (6 min) with 2-[^{3}H]deoxyglucose (0.1 mM final concentration). After final incubation, cultures were washed with phosphate-buffered saline, counted for radioactivity, and normalized against protein.

Immunoblotting and Signal Transduction Analyses—A group of eight KO mice were injected with PST (20 μg/g of body weight intraperitoneally twice daily) for 7 days. On the 8th day,

WT, KO, and KO + PST mice ($n = 4$ in each group) were fasted for 12 h and injected either with vehicle or with insulin (0.4 milliunits/g of body weight intraperitoneally). Mice were sacrificed after 20 min of treatment to collect tissues, which were snap frozen in liquid nitrogen. Tissues from vehicle-treated mice were considered as basal. Frozen tissues were homogenized in liquid nitrogen and lysed in a lysis buffer containing phosphatase and protease inhibitors as described elsewhere (17). Antibodies were purchased from Cell Signaling Technology (Beverly, MA) and Santa Cruz Biotechnology (Santa Cruz, CA). The chemiluminescence kit from Pierce was used for detection of signals.

Real Time PCR—RNA was extracted using an RNA purification kit (RNeasy Plus, Qiagen, Valencia, CA) according to the manufacturer's specifications. After DNase digestion, 100 ng of RNA was transcribed into cDNA in a 20-μl reaction using a High Capacity cDNA Archive kit, analyzed, and amplified. PCR was performed in a 25-μl reaction containing 5 μl of cDNA (one-fifth diluted), 2× SYBR Green PCR Master Mix, and a 400 nM concentration of each primer. Cycle threshold (Ct) values were used to calculate the amount of amplified PCR product relative to glyceraldehyde-3-phosphate dehydrogenase and 18 S rRNA.

PI 3-Kinase Assay—Primary hepatocytes were preincubated with 10 μM myristoylated conventional PKC (cPKC) peptide inhibitor (cPI; myr-RFARKGALRQKNV; Promega) for 1 h followed by incubation with PST (100 nM) for 30 min and then with insulin (20 nM) for 15 min. Hepatocytes were chilled, washed with cold phosphate-buffered saline, and then lysed in radioimmune precipitation assay buffer containing 1% Nonidet P-40 and protease and phosphatase inhibitors (all from Sigma) as described by Backer *et al.* (18). An aliquot of 500 μg of total cell protein extract used for each reaction was immunoprecipitated in lysis buffer with 4 μg of anti-insulin receptor substrate (IRS) 1/2 antibody (Upstate Biotechnology Inc). Immunoprecipitates were washed and analyzed for PI 3-kinase activity as described by Backer *et al.* (18).

cPKC Assay—We purchased peptide inhibitors PKCθ pseudosubstrate (sc-3097), PKCζ pseudosubstrate (sc-3098), PKCϵ peptide inhibitor (sc-3095), and PKCα peptide inhibitor (C2–4) (sc-3094) from Santa Cruz Biotechnology and non-peptide inhibitors LY333531 (IC_{50} for PKCβI and PKCβII, 5–6 nM), rottlerin (IC_{50} for PKCδ, 4 nM), and Gö6976 (IC_{50} for PKCα and PKCβ, 3–6 nM) from Calbiochem. Primary hepatocytes and HepG2 cells were incubated with 10 μM peptide inhibitors, 10 μM cPI, and 10 nM non-peptide inhibitors for 1 h followed by incubation with PST 100 nM for 15 min. After treatment, cells were chilled, washed, and lysed as described above. The kinase reaction mixture (120 μl) contained 20 mM Tris-HCl, pH 7.5, 10 mM $MgCl_2$, 0.5 mM $CaCl_2$, 25 μM phosphatidylserine, 6 μM [γ-^{32}P]ATP (5000–8000 cpm/pmol), and 25 μM peptide substrate derived from neurogranin (Santa Cruz Biotechnology). In some assays, PMA (1 μM) or 1:2 diolein (10 μM) was used as diacylglycerol. Reactions were initiated by the addition of [γ-^{32}P]ATP, proceeded for 10 min at 30 °C with linear kinetics, and were terminated by spotting on phosphocellulose papers. Papers were washed six times with 5% acetic acid. The radioactivities on the papers were analyzed by counting. All assays were performed in six replicates and expressed as the mean value ±S.E.

Statistics—Data are expressed as the mean ± S.E. Curve fitting was accomplished in the program Kaleidagraph (Synergy Software, Reading, PA). Multiple comparisons were made using either one-way ANOVA followed by Bonferroni's post hoc test or two-way ANOVA. Statistical significance was concluded at $p < 0.05$.

RESULTS

Body Composition and Plasma Lipid and Adipokine Profile—The gain in body weight (Fig. 1*A*) and total fat mass were 20 and 25%, respectively (Fig. 1*B*) in 6-month-old KO mice. After adjusting for increased body weight, the gain in fat mass was 25% of the gain in body weight. Total abdominal fat was also increased (by ~48%) predominantly at the epididymal and subepidermal regions and surrounding the adrenal gland (Fig. 1, *C* and *D*). Relative to WT, plasma triglyceride, NEFA, and IL-6 levels were lower (Fig. 1, *E–G*), whereas those of adiponectin and leptin (adjusted to fat mass) were higher in KO mice (Fig. 1*G*). Because IL-6 was shown to be elevated in patients with Type 2 diabetes mellitus (19) and adiponectin was shown to improve insulin sensitivity (20, 21), these findings correlate well with the data on hypertensive KO mice (decreased IL-6 and increased adiponectin levels), suggesting increased insulin sensitivity. The increase in fat mass may result from elevated lipid uptake and storage.

Insulin Metabolism and Action—Basal insulin levels were markedly (79%) lower in KO than WT mice (Fig. 2*A*). This is attributed to enhanced insulin clearance (as suggested by the ~6-fold increase in the steady state C-peptide/insulin ratio; Fig. 2*B*) but not reduced insulin secretion (as suggested by intact plasma C-peptide levels; Fig. 2*A*). The rapid initial rise in insulin levels during the first 7 min postglucose administration (Fig. 2*C*) suggests that the insulin secretion rate in response to glucose may instead be twice as high in KO mice lacking PST *versus* WT (0.107 *versus* 0.057 ng/ml/min in WT; $p < 0.05$) (Fig. 2*C*). Although actual assessment of insulin secretion by intravenous GTT was not carried out, a number of previous publications, either in perfused pancreas or in isolated beta cells, have demonstrated that PST inhibits the first phase of glucose-induced insulin secretion primarily by inhibiting a G-protein-coupled rise in calcium (22–25). Therefore, mice with PST deficiency might have enhanced insulin secretion during GTT.

Despite lower basal insulin levels (Fig. 2*A*), fasting blood glucose levels were normal in KO as compared with WT mice (Fig. 2*A*). Moreover insulin (Fig. 2*C*; area under the curve, 71.0 ± 6.6 *versus* 34.4 ± 9.5 ng/min/dl in WT; $p < 0.008$) and glucose (Fig. 2*D*; area under the curve, 5462.5 ± 582.3 *versus* 7918.8 ± 532 mg/min/dl in WT; $p < 0.009$) excursions in response to glucose challenge during an intraperitoneal GTT were significantly improved. This suggests that KO mice are insulin-sensitive.

In an ITT in 3-month-old mice, hypoglycemia was comparable between WT (51%) and KO (50%) mice (Fig. 2*E*), which returned to the basal level 120 min after insulin injection. In 6-month-old WT mice, hypoglycemia during ITT was lesser (by 11%), and the recovery from hypoglycemia was faster (90

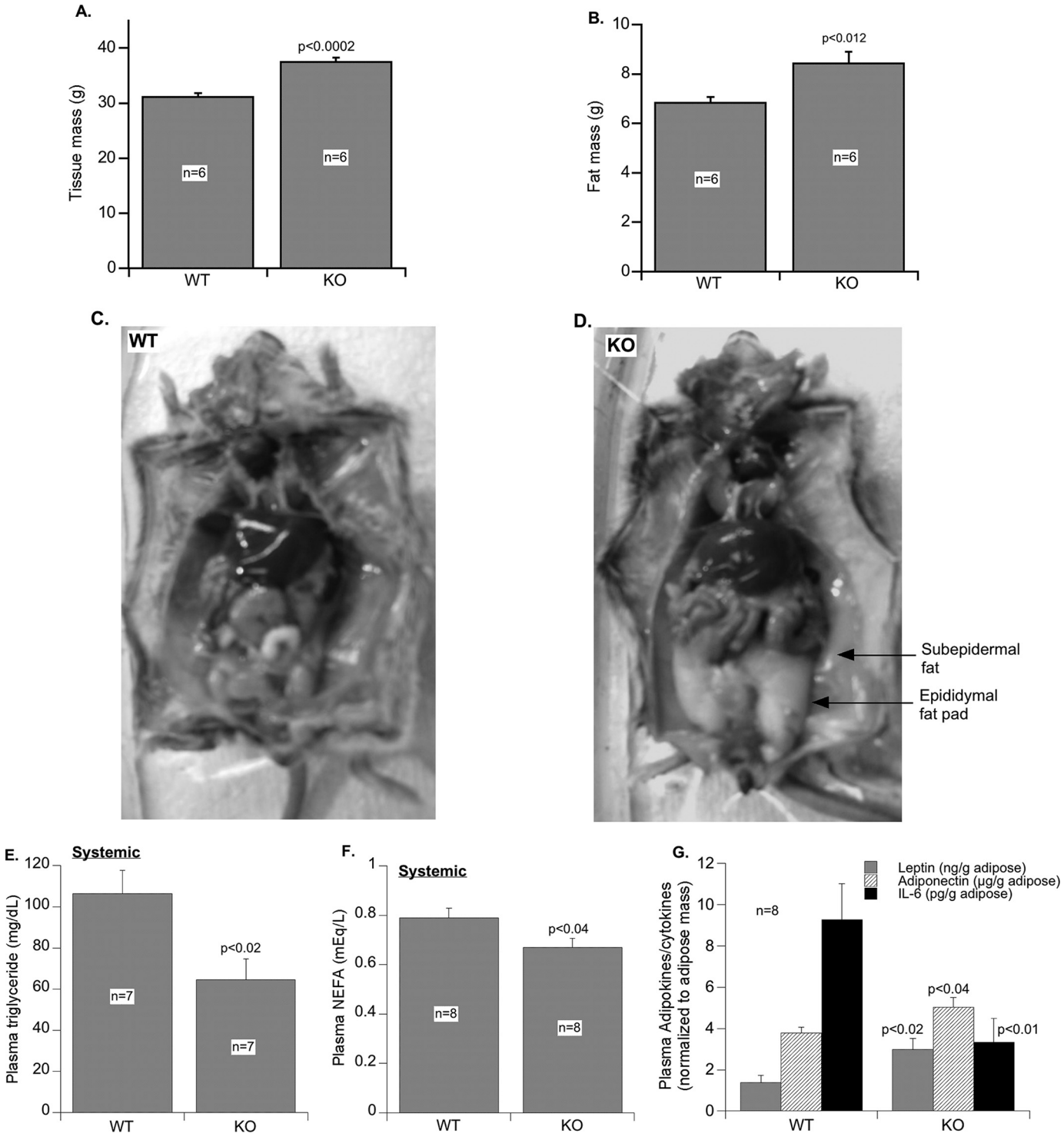

FIGURE 1. **Body composition, adipose tissue, and plasma adipocytokines.** 6-month-old male mice were fasted for 12 h before being subjected to a dual energy x-ray absorptiometry scan to measure total tissue mass (*A*) and total fat mass (*B*). A photograph of the intra-abdominal cavity in WT (*C*) and KO (*D*) mice reveals fat deposition in the epididymal and subepidermal regions. *E*, plasma triglyceride in 12-h fasted mice. *F*, plasma NEFA in 12-h fasted mice. *G*, plasma adipokine and cytokine levels in 12-h fasted mice. Experiments were performed on $n \geq 6$ per group. *A*, *B*, *E*, and *G*, values are expressed as mean ± S.E. ($p < 0.05$ *versus* WT).

min) as compared with 3-month-old mice (Fig. 2*F*). In contrast, in 6-month-old KO mice, although hypoglycemia was comparable between 3- and 6-month-old mice, the blood glucose did not return to the control level even after 150 min of insulin injection (Fig. 2*F*). This could be attributed to elevated glucose disposal and/or reduced gluconeogenesis in KO mice.

In response to glucose challenge, the plasma glucagon level dropped to a similar extent in WT (by 14.8%) and KO (by 17.6%) mice (Fig. 2*F*). This rules out a potential differential regulation of insulin action by glucagon in KO and WT mice.

Insulin Action in Vivo: Hyperinsulinemic-Euglycemic Clamp—Fasting blood glucose was slightly lower in WT *versus* KO mice

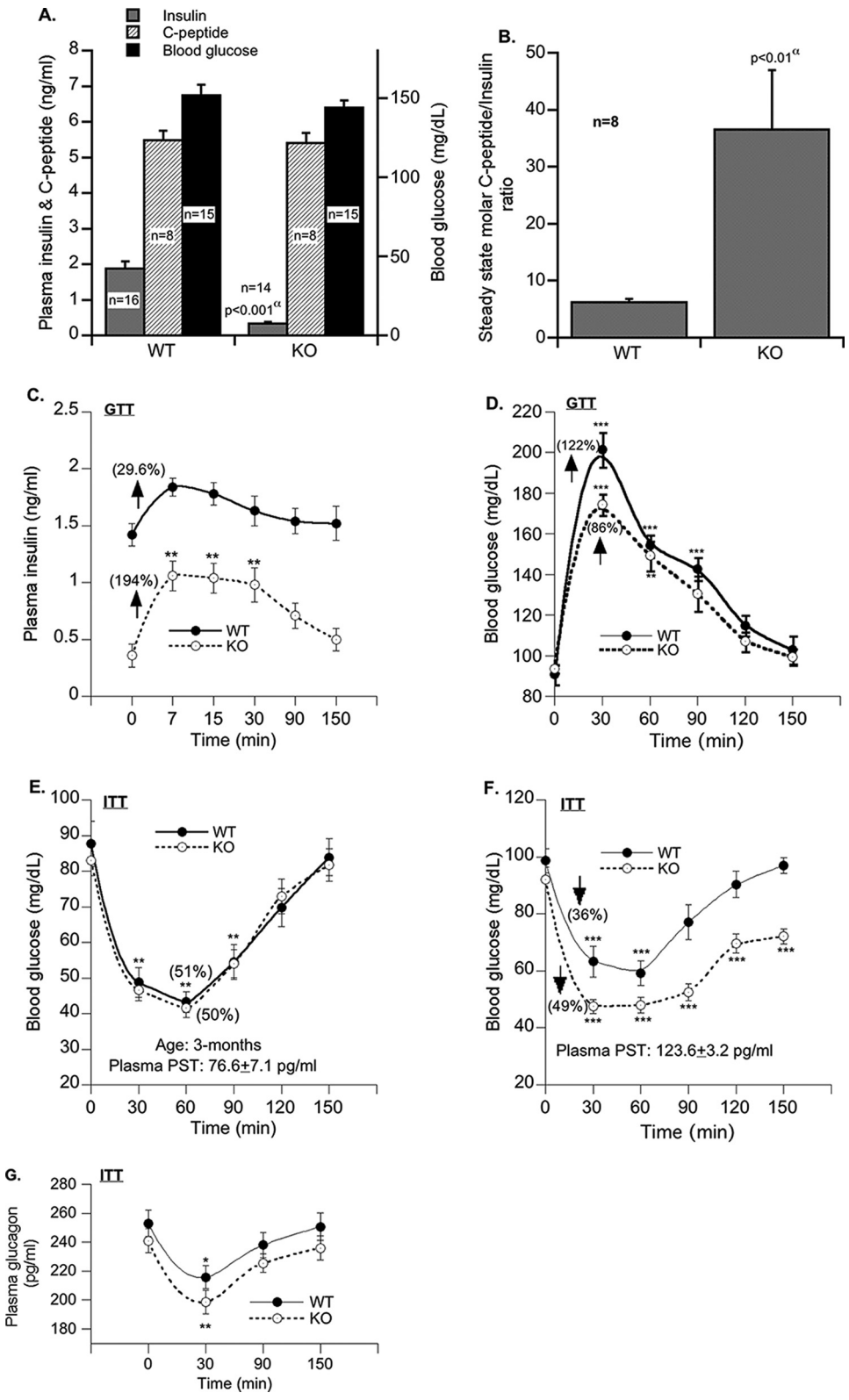

FIGURE 2. **Metabolic parameters in fasting (12 h) mice.** *A*, fasting blood glucose, plasma insulin and C-peptide levels. *B*, C-peptide/insulin molar ratio at steady state. Plasma insulin levels (*C*) and blood glucose during GTT (*D*) in fasting mice are shown (performed on $n = 8$ and analyzed by two-way ANOVA). Fasting blood glucose in 3-month-old mice (*E*), fasting blood glucose in 6-month-old mice (*F*), and fasting plasma glucagon during ITT (*G*) are shown (performed on $n = 8$ and analyzed by two-way ANOVA). Values are expressed as mean ± S.E. α, WT *versus* KO. *, $p < 0.05$; **, $p < 0.01$; ***, $p < 0.001$ as compared with the basal level.

(Fig. 3*A*). During the clamp, a steady state blood glucose concentration of ~120 mg/dl was reached at ~70 min and was maintained until the clamp was completed at 130 min. Blood glucose was maintained at a steady state level. Fig. 3*B* demonstrates that the specific activity of the tracer was in steady state at the end of the clamp, although the specific activity was significantly higher in KO *versus* WT at the end of the clamp period ($p < 0.05$). There was no difference in specific activity during the basal infusion period.

The overall glucose infusion rate required to maintain euglycemia during the clamp was comparable in WT and KO mice (Fig. 3*C*), suggesting that whole body insulin sensitivity was comparable between groups. However, the total glucose disposal rate during the clamp (GDR_{total}) was 35% lower in KO *versus* WT mice (Fig. 3*D*). In line with this, the insulin-stimulated GDR (which is calculated as $GDR_{clamp} - GDR_{basal}$), which primarily represents glucose disposal by skeletal muscle, was reduced by ~68% in KO compared with WT mice (Fig. 3*E*; $p < 0.006$). This finding is surprising given the positive effect of adiponectin on glucose transport in muscle (26, 27) and L6 muscle cells (Fig. 3*G*). Nonetheless these data indicate that, *in vivo*, KO mice develop insulin resistance in skeletal muscle.

In contrast to the insulin resistance in skeletal muscle, hepatic insulin sensitivity was significantly higher in KO mice compared with WT mice as evidenced by a greater suppression (by 32.2%) of hepatic glucose production during the clamp (Fig. 3*F*; $p < 0.0001$). Fasting hepatic glucose production/GDR was not different between groups (WT *versus* KO, 20 ± 2 *versus* 24 ± 3 mg/kg/min; p value not significant). The improved hepatic insulin sensitivity could, at least in part, be due to higher adiponectin levels (28, 29). Moreover the improved hepatic insulin sensitivity likely compensates for the muscle insulin resistance found in the KO mice and thus

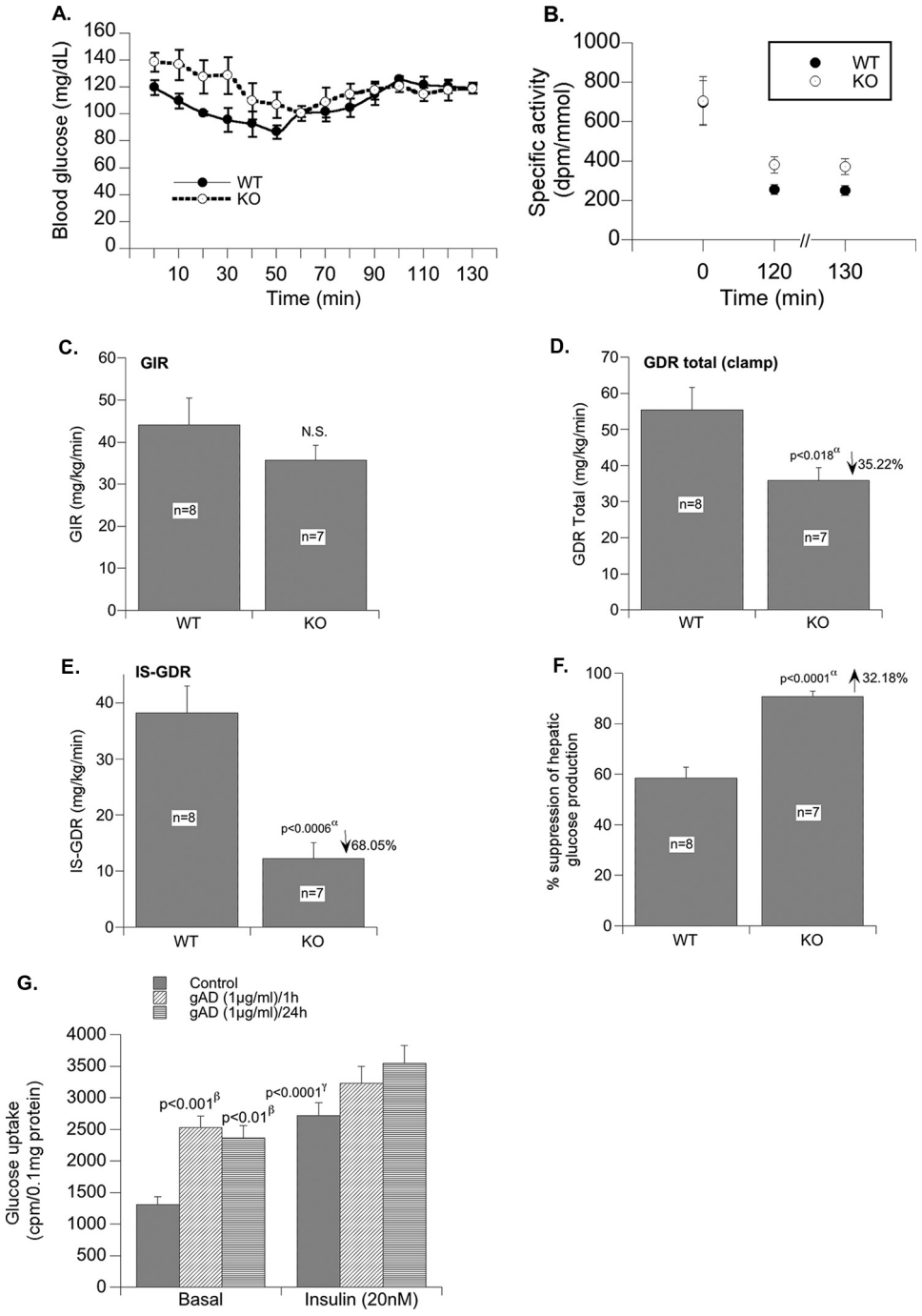

FIGURE 3. **Hyperinsulinemic-euglycemic clamp.** *A*, blood glucose concentrations during clamp. *B*, specific activity of [^{3}H]glucose in plasma during the basal/fasted (time, "0" min) state and the clamp (time, "120" and "130" min). *C*, glucose infusion rate (*GIR*) during the clamp. *D*, total glucose disposal rate (GDR_{total}) during the clamp. GDR in the basal/fasted state was not different between groups. *E*, insulin-stimulated GDR (*IS-GDR*). *F*, percent suppression of hepatic glucose production during the clamp. *G*, effect of globular adiponectin (*gAD*) on glucose uptake in cultured myotubes (L6). Values are expressed as mean ± S.E. α, WT *versus* KO; β, basal control *versus* gAD; γ, basal control *versus* insulin-treated control. *N.S.*, not significant.

contributes to the preserved euglycemic phenotype of the KO mouse. Increased insulin receptor activity may also contribute as we saw increased basal Tyr(P)-insulin receptor signaling in liver (results not presented).

Reduced Hepatic Gluconeogenesis in KO Mice—A reduction in hepatic gluconeogenesis in KO mice is further supported by a marked decrease in glucose production in response to pyruvate (Fig. 4*A*; area under the curve, 1738 ± 405 *versus* 3612 ± 393 mg/min/dl in WT mice; $p < 0.006$). Moreover mRNA levels of gluconeogenic genes, such as *Pepck1* and *G6pase*, were 61.0–71% lower in KO than WT mice (Fig. 4*B*). Conversely pretreatment of KO mice with PST restored *Pepck1* and *G6pase* mRNA levels (Fig. 4*B*) and glucose production in response to pyruvate (Fig. 4*A*). Together with higher hepatic glycogen content (Fig. 4*C*), which is in part mediated by reduced glycogenolysis, these results emphasize higher insulin sensitivity in KO mice.

Lipid Metabolism in KO Mice—The mRNA levels of lipogenic genes such as *Srebp1c*, *Pparγ*, and *Gpat* were high in KO mice and were conversely reduced by PST treatment (Fig. 4*D*). There was no significant change in *Fasn* expression between WT and KO mice (Fig. 4*D*). However, hepatic triglyceride content was intact (Fig. 4*C*). This could, at least in part, be due to elevated fatty acid β-oxidation in KO mice as suggested by higher levels of ketone bodies (Fig. 4*E*), phosphorylated acetyl-CoA carboxylase (Fig. 4*F*), and uncoupling protein 2 gene (*Ucp2*) (Fig. 4*G*). Increased ketone bodies point to diversion of the fatty acid oxidation product, acetyl-CoA, to ketogenesis.

Increased fatty acid oxidation could also underlie reduction in plasma NEFA levels (Fig. 1*F*). Lower plasma triglyceride levels (Fig. 1*E*) together with increased abdominal obesity suggest potential redistribution of lipid to the adipose tissue for storage.

PST (Human CHGA-(250–301)) Supplementation Reduces Insulin Sensitivity—The basal plasma PST level dropped significantly (by 12%) 30 min following insulin injection before it returned to normal (Fig. 5*A*), indicating an inverse relationship between plasma PST and insulin. In primary hepatocytes, PST effectively antagonizes the suppressive effect of insulin on glucose production from lactate and pyruvate (Fig. 5*B*). The restoration of mRNA levels of gluconeogenic genes (Fig. 4*B*) and glucose production in response to pyruvate in KO mice by PST treatment (Fig. 4*A*)

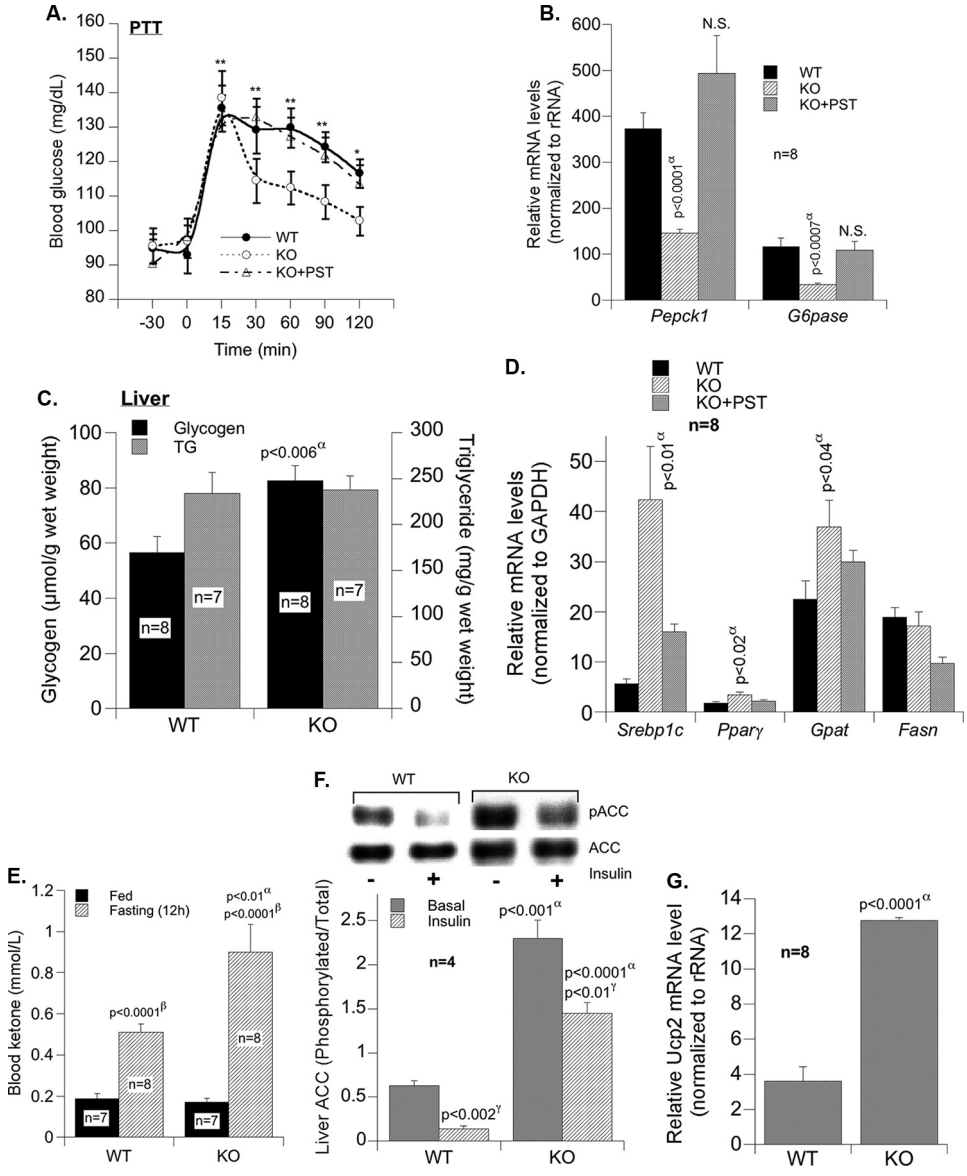

FIGURE 4. **Reduced hepatic gluconeogenesis in KO mice.** *A*, fasting (12 h) blood glucose during the pyruvate tolerance test (*PTT*) before and after pretreatment with PST. Experiments were analyzed as above (WT *versus* KO, $p < 0.005$; KO *versus* KO + PST, $p < 0.01$; WT *versus* KO + PST, $p = 0.84$). *B*, expression of gluconeogenic genes (*Pepck1* and *G6pase*) in liver. *C*, hepatic triglyceride and glycogen content in fasting (12 h) mice. *D*, expression of lipogenic genes (*Srebp1c*, *Pparγ*, *Gpat*, and *Fasn*) before and after PST treatment. *E*, blood ketone in fed and fasted (12 h) mice. *F*, Western analysis of phosphorylated acetyl-CoA carboxylase (*pACC*) in liver tissues. *G*, real time PCR analysis of the mRNA levels of hepatic *Ucp2*. α, WT *versus* KO; β, fed *versus* fasting; γ, basal *versus* insulin. Values are expressed as mean ± S.E. *, $p < 0.05$; **, $p < 0.01$ (comparison with zero time point). *N.S.*, not significant.

prompted us to further investigate the effect of PST on insulin action in KO mice.

Acute intraperitoneal injection of PST (40 μg/g of body weight) raised basal plasma PST levels from 0 to 162.9 ± 13.5 pg/ml in KO and from 125.0 ± 5.4 to 151.7 ± 9.1 pg/ml in WT mice. Whereas PST (40 μg/g) did not significantly alter the response of blood glucose levels to insulin injection in WT mice, it markedly reduced the effect of insulin on glucose disposal in KO mice (Fig. 5*C*). PST exerted no or a moderate effect on insulin tolerance at 10 and 20 μg/g of body weight, respectively (not shown).

Chronic PST treatment (20 μg/g intraperitoneally daily for 7 days) raised plasma PST from 0 to 154.1 ± 5.7 pg/ml in KO mice and caused insulin intolerance and resistance with blood glucose levels remaining high in the presence of insulin (Fig. 5*D*). Similar to native PST, the naturally occurring human variant of PST (G297S) (9) reduced insulin response although to a lesser extent and at twice the dose (Fig. 5*E*).

We determined the contribution of PST to the KO phenotype. PST increased hepatic glucose production in primary hepatocytes (Fig. 5*B*) and *in vivo* (Fig. 5, *C–E*). PST also impaired glucose uptake (insulin-stimulated) and leptin production in primary adipocyte cultures (Fig. 5, *F* and *G*) and *in vivo* (Fig. 5*H*). Interestingly PST failed to modulate insulin sensitivity in muscle cell cultures (Fig. 5*I*). This indicates that muscle insulin resistance was not caused by PST deficiency. It has been shown previously (8, 30) that PST inhibits insulin-stimulated glucose uptake in adipocytes, which we reconfirmed (Fig. 5*F*). As presented in Fig. 5, *G* and *H*, PST also inhibited leptin production, which possibly contributes to the higher levels of adipokines in *Chga*-KO mice (Fig. 1*G*). This is further supported by our present finding that replacement of PST in KO mice reduced circulating leptin level (Fig. 5*H*).

Signaling in Hepatic Tissues—Insulin signaling is enhanced in KO mice as indicated by induction of IRS1/2 and Akt phosphorylation (and activation) (Fig. 6, *A* and *B*, respectively). Consistent with the antagonistic effect of PST on insulin, PST markedly suppressed insulin signaling through IRS1/2 and Akt in KO mice. The higher levels of IRS1/2 and Akt phosphorylation in the absence of insulin may be due to activation of other receptor or non-receptor kinases (such as platelet-derived growth factor receptor and Src kinase), signals that are not significantly modulated by PST. Obviously deficiency of other Chga-derived peptides in KO mice may also evoke signaling responses that would be different from PST. For example, inhibition of tyrosine phosphatases by other peptides may raise basal signals for Tyr(P)-IRS2, whereas PST is involved with inhibition of insulin-stimulated signaling (not in muscle). Akt is phosphorylated by PDK1 and PDK2 (mTORC2). The products of PI 3-kinase activity activate PDK1. PI 3-kinase, in turn, is activated by a number of receptor tyrosine kinases (insulin recep-

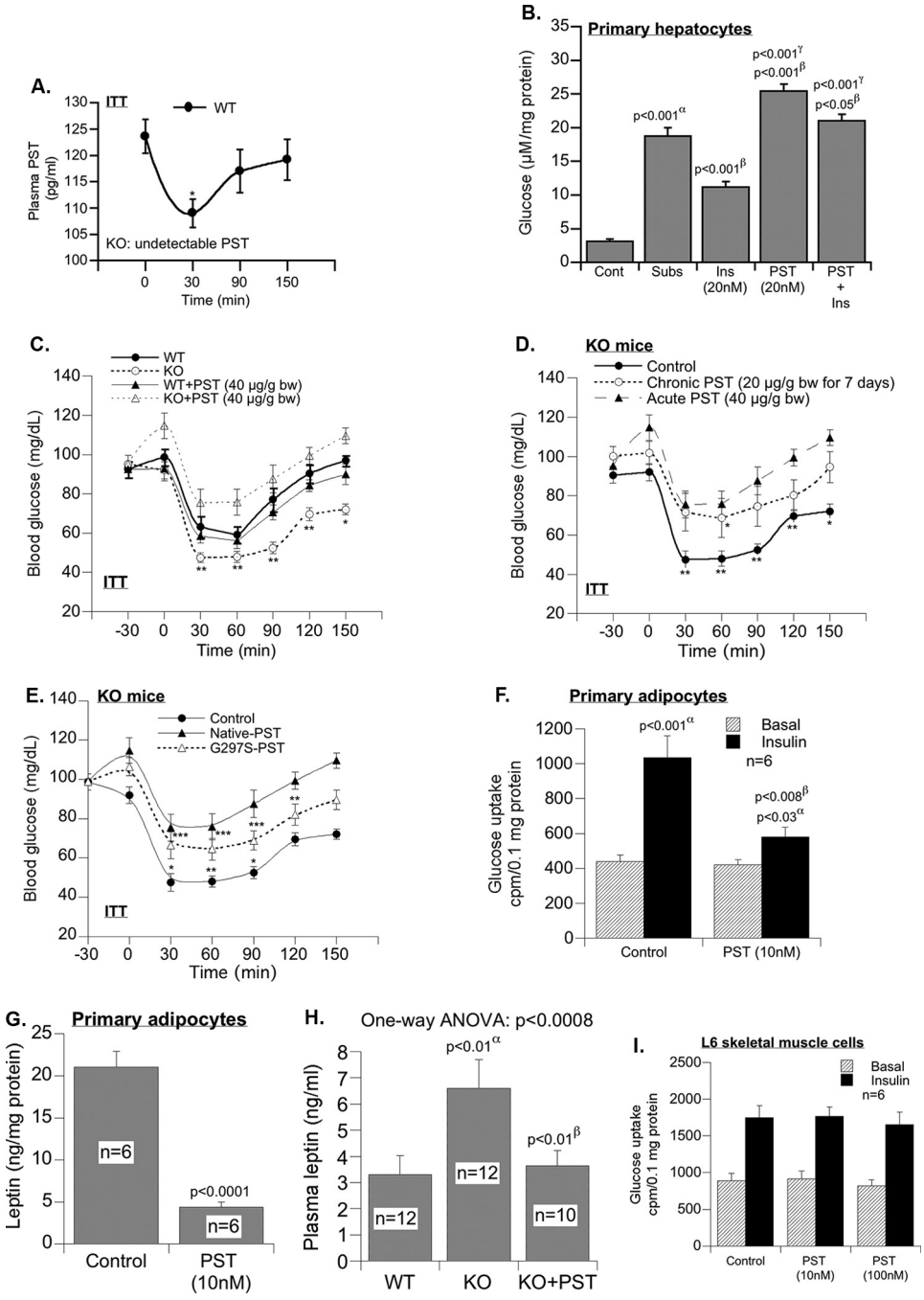

FIGURE 5. **PST supplementation abolishes heightened sensitivity to insulin.** *A*, fasting (12 h) plasma PST during ITT in WT mice showing an inverse correlation with insulin (one-way ANOVA ($n = 8$), $p < 0.046$). *B*, effect of PST on glucose production in primary hepatocytes. α, control *versus* substrate; β, substrate *versus* insulin, PST, or insulin plus PST; γ, insulin *versus* PST or insulin plus PST. *C*, fasting (12 h) blood glucose in WT and KO mice with or without PST 30 min before ITT ($n = 8$). *D*, fasting (12 h) blood glucose level in KO mice in response to acute or chronic native PST 30 min prior to ITT (two-way ANOVA ($n = 8$): control *versus* acute PST, $p < 0.001$; control *versus* chronic PST, $p < 0.001$; acute *versus* chronic PST, $p < 0.01$). *E*, fasting (12 h) blood glucose level in KO mice in response to saline, native PST, or PST-G297S variant 30 min prior to ITT (two-way ANOVA ($n = 8$): control *versus* WT PST, $p < 0.001$; control *versus* G297S-PST, $p < 0.001$; WT PST *versus* G297S-PST, $p < 0.01$; one-way ANOVA ($n = 8$), $p < 0.0001$; one-way ANOVA followed by Bonferroni's post hoc test: *, $p < 0.05$; **, $p < 0.01$; ***, $p < 0.001$ *versus* basal). *F*, effect of PST (10 nM) on glucose uptake in cultured primary adipocytes of WT mice. α, basal *versus* insulin; β, control *versus* PST. *G*, effect of PST (10 nM) on leptin secretion from cultured primary adipocytes of WT mice. *H*, effects of chronic PST replacement in KO mice for 7 days on plasma leptin level. α, WT *versus* KO; β, KO *versus* KO + PST. *I*, effect of PST on insulin-stimulated glucose uptake in L6 skeletal muscle cells. *Cont*, control; *Subs*, substrate; *Ins*, insulin; *bw*, body weight.

tor, platelet-derived growth factor receptor, and epidermal growth factor receptor) and a non-receptor tyrosine kinase (Src kinase). Platelet-derived growth factor, epidermal growth factor receptor, and Src kinases do not use IRS1/2 for activation of PI 3-kinase and do not need insulin for activation. Basal phosphorylation (without insulin) of Akt can be achieved by many other ligands of tyrosine kinases and therefore may not be competed by PST.

In parallel to mRNA (Fig. 4*D*), the protein levels of mature SREBP1c were also elevated in KO mice in the absence but not the presence of PST (Fig. 6*C*). KO mice also exhibited higher levels of basal FOXO-1 phosphorylation in the absence than in the presence of PST. This is consistent with the negative role of SREBP1c and FOXO-1 phosphorylation on the expression of gluconeogenic genes (21, 22) and the reversal effect of PST on glucose production from pyruvate in KO mice (Fig. 4*A*).

Because the action of PST depends on the activity of cPKC (32), we tested whether cPKC inhibition protects insulin signaling against PST. As Fig. 6*E* reveals, cPI peptide effectively inhibited cPKC activity in the presence of insulin in PST-treated primary hepatocytes from WT mice. To further characterize PKC isoform specificity of PST, HepG2 cells were treated with 10 μM PKCθ pseudosubstrate, PKCζ pseudosubstrate, PKCϵ peptide inhibitor, and PKCα peptide inhibitor (C2–4) and a 10 nM concentration of the non-peptide inhibitors LY333531 (IC_{50} for PKCβI and PKCβII, 5–6 nM), rottlerin (IC_{50} for PKCδ, 4 nM), and Gö6976 (IC_{50} for PKCα and PKCβ, 3–6 nM). Inhibitors of PKCα and PKCβ (sc-3094, LY333531, and Gö6976) blocked PST-induced PKC activity. Our results demonstrated that PST-induced effects work primarily through a PKCα and PKCβ pathway (Fig. 6*F*), confirming our earlier conclusion and supporting previously published results that classical

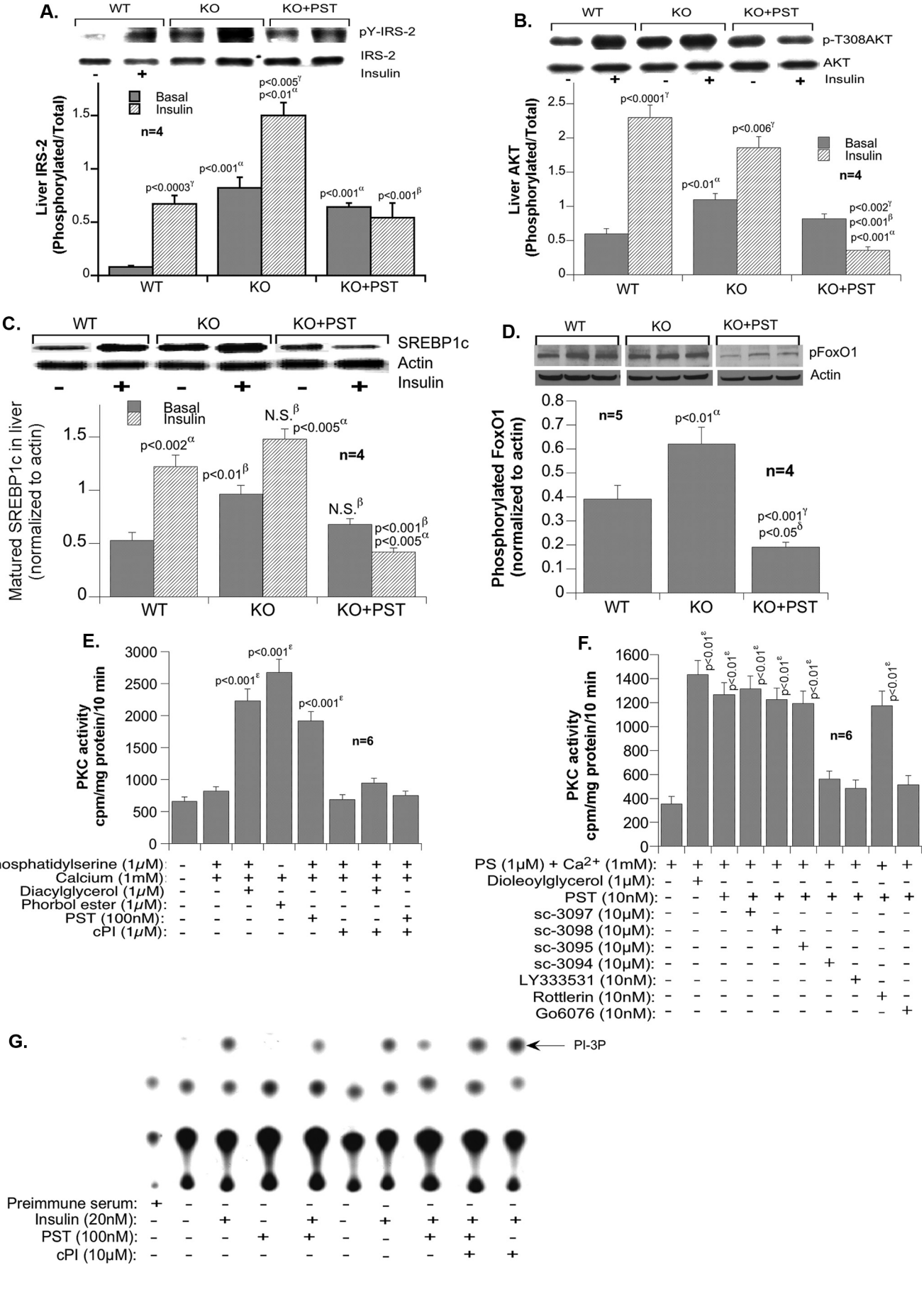
A.
WT
KO
KO+PST
pY-IRS-2
IRS-2
Insulin
Basal
Insulin
n=4
Liver IRS-2 (Phosphorylated/Total)
p<0.0003γ
p<0.001α
p<0.005γ
p<0.01α
p<0.001α
p<0.001β
B.
p-T308AKT
AKT
Liver AKT (Phosphorylated/Total)
p<0.0001γ
p<0.01α
p<0.006γ
p<0.002γ
p<0.001β
p<0.001α
C.
SREBP1c
Actin
Matured SREBP1c in liver (normalized to actin)
p<0.002α
p<0.01β
N.S.β
p<0.005α
N.S.β
p<0.001β
p<0.005α
D.
pFoxO1
Actin
Phosphorylated FoxO1 (normalized to actin)
n=5
p<0.01α
p<0.001γ
p<0.05δ
E.
PKC activity cpm/mg protein/10 min
p<0.001ε
n=6
Phosphatidylserine (1μM)
Calcium (1mM)
Diacylglycerol (1μM)
Phorbol ester (1μM)
PST (100nM)
cPI (1μM)
F.
PKC activity cpm/mg protein/10 min
p<0.01ε
n=6
PS (1μM) + Ca2+ (1mM)
Dioleoylglycerol (1μM)
PST (10nM)
sc-3097 (10μM)
sc-3098 (10μM)
sc-3095 (10μM)
sc-3094 (10μM)
LY333531 (10nM)
Rottlerin (10nM)
Go6076 (10nM)
G.
PI-3P
Preimmune serum
Insulin (20nM)
PST (100nM)
cPI (10μM)

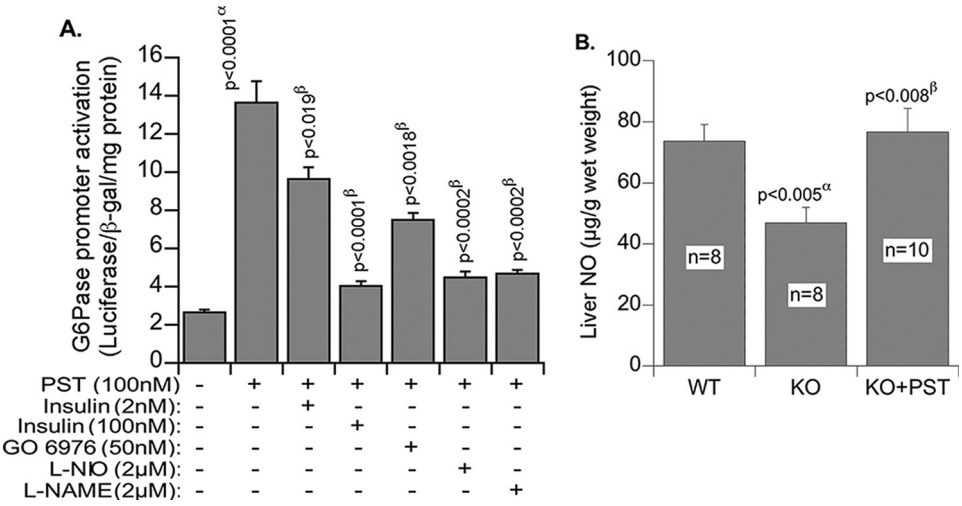

FIGURE 7. *A*, glucose-6-phosphatase expression in transfected HepG2 cells. α, basal *versus* PST; β, PST *versus* PST + inhibitors. *B*, liver NO content in WT and KO mice. α, WT *versus* KO; β, KO *versus* KO + PST. *L-NIO*, N^5-(1-imino-3-butenyl)-L-ornithine; *L-NAME*, N^G-nitro-L-arginine methyl ester; *β-gal*, β-galactosidase. Values are expressed as mean ± S.E.

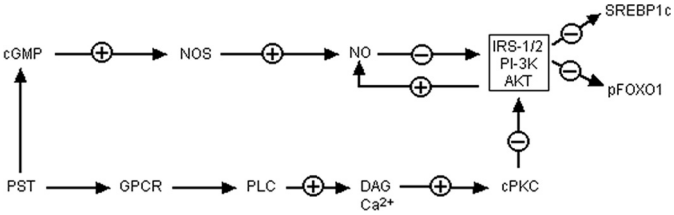

FIGURE 8. **Schematic diagram showing the mechanism of action of PST toward glucose homeostasis.** *GPCR*, G-protein-coupled receptor; *PLC*, phospholipase C; *DAG*, diacylglycerol; *PI-3K*, phosphatidylinositol 3-kinase; *pFOXO1*, phosphorylated FOXO-1.

PKCs are involved in PST action. PST significantly reduced insulin-stimulated PI 3-kinase activity in the anti-IRS1/2 immunopellet in the absence but not in the presence of cPI (Fig. 6*G*). This supports the notion that cPKC inhibition protects against the anti-insulin action of PST. These results corroborate previous reports that PST inhibits PI 3-kinase through cPKC (8) and imply that modulation of FOXO-1 and SREBP1c signaling by PST is mediated through inhibition of PI 3-kinase activity because these transcription factors require PI 3-kinase activity (33–36).

To gain a better insight into PST signaling and gluconeogenesis we transfected hepatocytes with G6Pase promoter fused with luciferase reporter and found ~6-fold activation of G6Pase expression by PST (Fig. 7*A*). Insulin suppressed PST-induced expression of G6Pase both at low (2 nM; by 30–35%) and high (100 nM; by 80%) concentrations. Chemical inhibition of NOS (N^5-(1-imino-3-butenyl)-L-ornithine and N^G-nitro-L-arginine methyl ester) and cPKC (Gö6976) also inhibited PST-induced expression of G6Pase by 80 and 50%, respectively. The hepatic NO level in *Chga* KO mice was diminished as compared with WT mice, and supplementation with PST restored NO to the WT level (Fig. 7*B*). The NOS inhibitor N^5-(1-imino-3-butenyl)-L-ornithine is known to be selective for eNOS, and its inhibitory effects on PST-stimulated promoter activation suggest that eNOS signaling may be required for the gluconeogenic effects of PST. The above findings suggest that PST might utilize two pathways for induction of gluconeogenesis, one by suppressing the PI 3-kinase-Akt-FOXO-1 (SREBP1) pathway and the other by activating the NOS pathway (Fig. 8).

DISCUSSION

Consistent with the antagonistic effect of the CHGA peptide PST on insulin action in adipocytes (8, 30, 37) and hepatocytes (32, 38), the current studies demonstrated that *Chga* KO mice display *increased* insulin sensitivity as confirmed by GTT (Fig. 2*D*), ITT (Fig. 2*E*), clamp studies (Fig. 3, *D–F*), and pyruvate tolerance test (Fig. 4*A*). Conversely PST administration reversed insulin sensitivity in these mice (Fig. 4, *A* and *B*).

Insulin reduced the plasma PST level in WT mice (Fig. 5*A*), and lack of PST did not raise the insulin level (Fig. 2*A*). Consistent with the inhibitory effect of PST on insulin secretion in isolated rat pancreas (3), the glucose-stimulated insulin secretion rate and the area under the curve of insulin release during GTT were elevated in KO mice (Fig. 2*C*). However, steady state insulin level remained lower in KO than in WT mice. This appears to be due to enhanced insulin clearance as suggested by the higher level of steady state molar C-peptide/insulin ratio (Fig. 2*B*) (39). A positive link between insulin sensitivity and enhanced insulin extraction has been widely observed in humans (40). Nevertheless it should be noted that PST did not appear to modulate this effect because PST replacement in *Chga* KO mice did not raise insulin levels to those seen in WT mice (results not shown). Further studies to explore the mechanisms underlying a potential regulation of insulin clearance by the CHGA-derived peptides are needed.

Because the liver and adipose tissue did not express PST (data not shown), our data suggest an endocrine regulation by this peptide. In WT mice, plasma PST level increased with age, rising from 76.6 ± 7.1 to 123.6 ± 3.2 pg/ml at 3–6 months (Fig. 2, *E* and *F*). Thus, the rise in PST levels occurs in parallel to reduced insulin tolerance and hence insulin action. *In vivo* studies further suggest that the main antagonistic effect of PST on insulin action is to reduce the suppressive effect of insulin on hepatic gluconeogenesis (Fig. 4, *A* and *B*). Administration of

FIGURE 6. **Signaling in liver.** Immunoblot analysis of the phosphorylation of IRS2 (*pY-IRS-2*) (*A*) and Akt (*p-T308AKT*) (*B*) in liver tissues is shown. The experiments were performed on four mice per group and scanned, and the band density was analyzed by one-way ANOVA. *C*, Western analysis of mature SREBP1c protein content in liver with and without PST pretreatment. *D*, Western analysis of the phosphorylation of FOXO-1 (*pFoxO1*) in liver with and without PST pretreatment. *E*, cPKC activity in primary hepatocytes in response to PST. *F*, effects of isoform-selective inhibition of PST-stimulated PKC activities in HepG2 cells. *G*, the effect of PST on insulin-stimulated PI 3-kinase (*PI-3P*) activity. *A–F*, values are expressed as mean ± S.E. α, WT *versus* KO; β, KO *versus* KO + PST; γ, basal *versus* insulin; δ, WT *versus* KO + PST. ***, $p < 0.001$ *versus* control. *N.S.*, not significant; *PS*, phosphatidylserine.

PST to KO mice raised the glucose level even higher than in WT (Fig. 5*C*). Consistently PST increased mRNA levels of *Pepck1* and *G6pase* gluconeogenic genes (Fig. 4*B*).

Based on our data, we suggest that the antagonistic effects of PST on insulin signaling via the Akt/FOXO-1 (Fig. 6, *B* and *D*) and SREBP1c (Fig. 6*C*) gluconeogenic pathways are mediated by cPKC-dependent inactivation of PI 3-kinase activity. This is supported by the protective effect of cPI on insulin-stimulated PI 3-kinase activity against PST (Fig. 6*G*). PI 3-kinase activity is crucial for FOXO-1- (33, 41) and SREBP1c (34–36)-mediated regulation of gluconeogenesis. There is also a second component to PST action that is mediated by the eNOS/NO pathway (Fig. 7). Inhibitors of eNOS blocked PST action on gluconeogenesis. The NO/NOS signaling pathway plays a very subtle and delicate role in glucose metabolism and insulin resistance. A small amount of NO is needed for vascular relaxation and for maintaining improved blood flow. But excessive NO accumulation can cause metabolic damage. Thus, the effects of NO burst via inducible NOS, which is observed during septic shock and inflammation, could be deleterious, and therefore, inactivation of inducible NOS by L-N^6-(1-iminoethyl)lysine treatment or knocking out inducible NOS gene improves insulin sensitivity (42, 43). On the other hand, depletion of NO through deletion of ubiquitous eNOS provokes insulin resistance (44). However, reversible suppression of NOS activity by N^G-nitro-L-arginine methyl ester protects against high fat diet-induced insulin resistance possibly through increased fatty acid disposal (45, 46). One of the effects of NO-mediated damage is created by reversible inactivation of IRS1/Akt-mediated signaling via *S*-nitrosylation (47, 48). Therefore, it is possible that the higher basal phosphorylated Akt and Tyr(P)-IRS1/2 signals observed in liver of *Chga* KO mice are the result of protection of those signals (from nitrosylation) due to low NO levels in KO mice. These results suggested that promotion of gluconeogenesis by PST might be mediated by two pathways, one by suppressing the PI 3-kinase-Akt-FOXO-1 (SREBP1) pathway and the other by activating the eNOS pathway. The combined effects of cPKC and eNOS activation by PST can suppress insulin signaling.

Because exclusion of phosphorylated FOXO-1 from the nucleus and overexpression of mature transcription factor SREBP1c suppress gluconeogenic gene transcription (49, 50), it is reasonable to conclude that constitutive phosphorylation of FOXO-1 by Akt and basal enhancement of SREBP1c maturation in the absence of PST decrease gluconeogenic gene expression and reduce hepatic glucose production in KO mice. Consistent with this conclusion, PST administration attenuated phosphorylated FOXO-1 and SREBP1c signals. These findings identify a novel role for PST "hormone" in the regulation of gluconeogenic gene transcription by insulin.

Additionally *Chga* deficiency appeared to promote lipid redistribution to the adipose depot for storage (Fig. 1, *C* and *D*) perhaps in response to increased insulin secretion. Whether lipid is being distributed to muscle is unclear, but an excess supply of fatty acids from the adipose tissue may also be transported to muscle as well as liver for oxidation. The lower NO level in KO mice may facilitate fatty acid oxidation, compete with glucose uptake, and decrease glucose disposal in muscle. Because NO has been shown to stimulate glucose uptake by muscle (51, 52) lower NO level itself may reduce muscle glucose disposal as seen in KO mice. Nevertheless insulin resistance in muscle failed to cause global insulin resistance in KO mice perhaps because of the development of compensatory mechanisms, such as up-regulation of glucose uptake in other tissues in the presence of elevated levels of adipokines, which regulate glucose disposal independently of insulin (26, 27), and reduction in hepatic glucose production. The chronically elevated state of hepatic ketogenesis in these mice (Fig. 4*E*) may lead to metabolic adaptation to fatty acid rather than glucose oxidation for fuel to prevent muscle protein breakdown (53, 54).

Alternatively it is possible that compromised glucose disposal in muscle occurs to prevent hypoglycemia, which may result from reduction in hepatic glucose production. It is intriguing that although catecholamines stimulate transient gluconeogenesis and glycogenolysis (55, 56) glucose production is low and hepatic glycogen content (Fig. 4*C*) is high in KO as compared with WT mice. This could be due in part to the suppressive effect of leptin on epinephrine-induced hepatic glucose production (57) and to the absence of PST-induced glycogenolysis (6, 31) in KO mice. Thus, glucose homeostasis in PST-deficient hypertensive *Chga* KO mice is maintained by (i) increased suppression of hepatic glucose production (contribution of PST deficiency and increased adipokine levels), (ii) increased glycogen accumulation in liver (contribution of PST deficiency), and (iii) adipokine-mediated glucose disposal by muscle. *Chga* deletion leads to deficiency of four known peptides, including Chga proprotein, resulting in multifactorial alterations in mouse phenotype. We attempted to isolate the contribution of PST to the observed phenotype found in mice with *Chga* gene deletion and demonstrated that PST affects insulin action in hepatocytes and adipocytes but not in muscle cells. The results in muscle cells are in line with clinical studies in human that found that infusion of PST into the forearm did not affect insulin-stimulated glucose metabolism compared with control infusion (9). Because of these results, we hypothesize that skeletal muscle insulin resistance in *Chga* KO mice is not due to PST deficiency.

In summary, lack of PST, despite elevated plasma catecholamines and corticosterone levels, increases insulin sensitivity and helps maintain euglycemia in KO mice by relieving inhibition from IRS1/2-PI 3-kinase-Akt signaling (achieved through suppression of cPKC and NOS activity) leading to increased suppression of hepatic gluconeogenesis (Fig. 8). Despite a low level of insulin (only 20% of WT) and the development of hypertension, which results from loss of catestatin (12), KO mice remained euglycemic. Because PST is overexpressed in Type 2 diabetes mellitus (10–12), our observations may have implications for the pathogenesis and treatment of diabetes. Our data propose that loss of PST in KO mice provides protection against possible hypertension-induced metabolic disorders.

Acknowledgment—Hyperinsulinemic-euglycemic clamp studies were conducted in the laboratory of Jerrold M. Olefsky at University of California, San Diego.

REFERENCES

1. Winkler, H., and Fischer-Colbrie, R. (1992) *Neuroscience* **49,** 497–528
2. Taupenot, L., Harper, K. L., and O'Connor, D. T. (2003) *New Engl. J. Med.* **348,** 1134–1149
3. Tatemoto, K., Efendiæ, S., Mutt, V., Makk, G., Feistner, G. J., and Barchas, J. D. (1986) *Nature* **324,** 476–478
4. Aardal, S., Helle, K. B., Elsayed, S., Reed, R. K., and Serck-Hanssen, G. (1993) *J. Neuroendocrinol.* **5,** 405–412
5. Mahata, S. K., O'Connor, D. T., Mahata, M., Yoo, S. H., Taupenot, L., Wu, H., Gill, B. M., and Parmer, R. J. (1997) *J. Clin. Investig.* **100,** 1623–1633
6. Sánchez-Margalet, V., Calvo, J. R., and Goberna, R. (1992) *Horm. Metab. Res.* **24,** 455–457
7. Sánchez-Margalet, V., Calvo, J. R., Lucas, M., and Goberna, R. (1992) *Gen. Pharmacol.* **23,** 637–638
8. González-Yanes, C., and Sánchez-Margalet, V. (2000) *Diabetes* **49,** 1288–1294
9. O'Connor, D. T., Cadman, P. E., Smiley, C., Salem, R. M., Rao, F., Smith, J., Funk, S. D., Mahata, S. K., Mahata, M., Wen, G., Taupenot, L., Gonzalez-Yanes, C., Harper, K. L., Henry, R. R., and Sanchez-Margalet, V. (2005) *J. Clin. Endocrinol. Metab.* **90,** 5414–5425
10. Sánchez-Margalet, V., Lobón, J. A., González, A., Fernández-Soto, M. L., Escobar-Jiménez, F., and Goberna, R. (1998) *Diabetes Care* **21,** 1951–1954
11. Funakoshi, A., Tateishi, K., Shinozaki, H., Matsumoto, M., and Wakasugi, H. (1990) *Regul. Pept.* **30,** 159–164
12. Mahapatra, N. R., O'Connor, D. T., Vaingankar, S. M., Hikim, A. P., Mahata, M., Ray, S., Staite, E., Wu, H., Gu, Y., Dalton, N., Kennedy, B. P., Ziegler, M. G., Ross, J., and Mahata, S. K. (2005) *J. Clin. Investig.* **115,** 1942–1952
13. Li, H. Y., Chiu, Y. F., Hwu, C. M., Sheu, W. H., Hung, Y. J., Fujimoto, W., Quertermous, T., Curb, J. D., Tai, T. Y., and Chuang, L. M. (2008) *Am. J. Hypertens.* **21,** 471–476
14. Seifter, S., and Dayton, S. (1950) *Arch. Biochem.* **25,** 191–200
15. Smedsrød, B., and Pertoft, H. (1985) *J. Leukoc. Biol.* **38,** 213–230
16. Karnieli, E., Zarnowski, M. J., Hissin, P. J., Simpson, I. A., Salans, L. B., and Cushman, S. W. (1981) *J. Biol. Chem.* **256,** 4772–4777
17. Hevener, A. L., Olefsky, J. M., Reichart, D., Nguyen, M. T., Bandyopadyhay, G., Leung, H. Y., Watt, M. J., Benner, C., Febbraio, M. A., Nguyen, A. K., Folian, B., Subramaniam, S., Gonzalez, F. J., Glass, C. K., and Ricote, M. (2007) *J. Clin. Investig.* **117,** 1658–1669
18. Backer, J. M., Schroeder, G. G., Kahn, C. R., Myers, M. G., Jr., Wilden, P. A., Cahill, D. A., and White, M. F. (1992) *J. Biol. Chem.* **267,** 1367–1374
19. Bastard, J. P., Jardel, C., Bruckert, E., Blondy, P., Capeau, J., Laville, M., Vidal, H., and Hainque, B. (2000) *J. Clin. Endocrinol. Metab.* **85,** 3338–3342
20. Minokoshi, Y., Kim, Y. B., Peroni, O. D., Fryer, L. G., Müller, C., Carling, D., and Kahn, B. B. (2002) *Nature* **415,** 339–343
21. Kadowaki, T., Yamauchi, T., Kubota, N., Hara, K., Ueki, K., and Tobe, K. (2006) *J. Clin. Investig.* **116,** 1784–1792
22. Efendiæ, S., Tatemoto, K., Mutt, V., Quan, C., Chang, D., and Ostenson, C. G. (1987) *Proc. Natl. Acad. Sci. U.S.A.* **84,** 7257–7260
23. Ahrén, B., Bertrand, G., Roye, M., and Ribes, G. (1996) *Acta Physiol. Scand.* **158,** 63–70
24. Ma, H. T., Kato, M., and Tatemoto, K. (1996) *Regul. Pept.* **61,** 143–148
25. Hertelendy, Z. I., Patel, D. G., and Knittel, J. J. (1996) *Cell Calcium* **19,** 125–132
26. Yamauchi, T., Kamon, J., Minokoshi, Y., Ito, Y., Waki, H., Uchida, S., Yamashita, S., Noda, M., Kita, S., Ueki, K., Eto, K., Akanuma, Y., Froguel, P., Foufelle, F., Ferre, P., Carling, D., Kimura, S., Nagai, R., Kahn, B. B., and Kadowaki, T. (2002) *Nat. Med.* **8,** 1288–1295
27. Ceddia, R. B., Somwar, R., Maida, A., Fang, X., Bikopoulos, G., and Sweeney, G. (2005) *Diabetologia* **48,** 132–139
28. Zhou, H., Song, X., Briggs, M., Violand, B., Salsgiver, W., Gulve, E. A., and Luo, Y. (2005) *Biochem. Biophys. Res. Commun.* **338,** 793–799
29. Combs, T. P., Berg, A. H., Obici, S., Scherer, P. E., and Rossetti, L. (2001) *J. Clin. Investig.* **108,** 1875–1881
30. Sánchez-Margalet, V., and González-Yanes, C. (1998) *Am. J. Physiol. Endocrinol. Metab.* **275,** E1055–E1060
31. Sánchez, V., Lucas, M., Calvo, J. R., and Goberna, R. (1992) *Biochem. J.* **284,** 659–662
32. Sánchez-Margalet, V., Lucas, M., and Goberna, R. (1994) *Biochem. J.* **303,** 51–54
33. Nakae, J., Park, B. C., and Accili, D. (1999) *J. Biol. Chem.* **274,** 15982–15985
34. Fleischmann, M., and Iynedjian, P. B. (2000) *Biochem. J.* **349,** 13–17
35. Azzout-Marniche, D., Bécard, D., Guichard, C., Foretz, M., Ferré, P., and Foufelle, F. (2000) *Biochem. J.* **350,** 389–393
36. Matsumoto, M., Ogawa, W., Teshigawara, K., Inoue, H., Miyake, K., Sakaue, H., and Kasuga, M. (2002) *Diabetes* **51,** 1672–1680
37. González-Yanes, C., Santos-Alvarez, J., and Sánchez-Margalet, V. (1999) *Biochim. Biophys. Acta* **1451,** 153–162
38. Sánchez-Margalet, V. (1999) *Diabetologia* **42,** 317–325
39. Poy, M. N., Yang, Y., Rezaei, K., Fernström, M. A., Lee, A. D., Kido, Y., Erickson, S. K., and Najjar, S. M. (2002) *Nat. Genet.* **30,** 270–276
40. Osei, K., Gaillard, T., and Schuster, D. (2007) *Metabolism* **56,** 24–29
41. Rena, G., Guo, S., Cichy, S. C., Unterman, T. G., and Cohen, P. (1999) *J. Biol. Chem.* **274,** 17179–17183
42. Perreault, M., and Marette, A. (2001) *Nat. Med.* **7,** 1138–1143
43. Fujimoto, M., Shimizu, N., Kunii, K., Martyn, J. A., Ueki, K., and Kaneki, M. (2005) *Diabetes* **54,** 1340–1348
44. Cook, S., Hugli, O., Egli, M., Ménard, B., Thalmann, S., Sartori, C., Perrin, C., Nicod, P., Thorens, B., Vollenweider, P., Scherrer, U., and Burcelin, R. (2004) *Diabetes* **53,** 2067–2072
45. Tsuchiya, K., Sakai, H., Suzuki, N., Iwashima, F., Yoshimoto, T., Shichiri, M., and Hirata, Y. (2007) *Endocrinology* **148,** 4548–4556
46. Joost, H. G., and Tschöp, M. H. (2007) *Endocrinology* **148,** 4545–4547
47. Yasukawa, T., Tokunaga, E., Ota, H., Sugita, H., Martyn, J. A., and Kaneki, M. (2005) *J. Biol. Chem.* **280,** 7511–7518
48. Carvalho-Filho, M. A., Ueno, M., Hirabara, S. M., Seabra, A. B., Carvalheira, J. B., de Oliveira, M. G., Velloso, L. A., Curi, R., and Saad, M. J. (2005) *Diabetes* **54,** 959–967
49. Yamamoto, T., Shimano, H., Nakagawa, Y., Ide, T., Yahagi, N., Matsuzaka, T., Nakakuki, M., Takahashi, A., Suzuki, H., Sone, H., Toyoshima, H., Sato, R., and Yamada, N. (2004) *J. Biol. Chem.* **279,** 12027–12035
50. Chakravarty, K., and Hanson, R. W. (2007) *Nutr. Rev.* **65,** S47–56
51. Lira, V. A., Soltow, Q. A., Long, J. H., Betters, J. L., Sellman, J. E., and Criswell, D. S. (2007) *Am. J. Physiol. Endocrinol. Metab.* **293,** E1062–E1068
52. Higaki, Y., Hirshman, M. F., Fujii, N., and Goodyear, L. J. (2001) *Diabetes* **50,** 241–247
53. Thompson, J. R., and Wu, G. (1991) *Comp. Biochem. Physiol. B* **100,** 209–216
54. Finn, P. F., and Dice, J. F. (2006) *Nutrition* **22,** 830–844
55. Saccà, L., Vigorito, C., Cicala, M., Corso, G., and Sherwin, R. S. (1983) *Am. J. Physiol. Endocrinol. Metab.* **245,** E294–E302
56. Sánchez-Gutierrez, J. C., Sánchez-Arias, J. A., Samper, B., and Felíu, J. E. (1997) *Endocrinology* **138,** 2443–2448
57. Roden, M. (2008) *Wien. Med. Wochenschr.* **158,** 558–561